MECHANISM OF INCIPIENT FLUIDIZATION IN FLUIDIZED BED AT ELEVATED TEMPERATURE

RYOHEI YAMAZAKI, NAOKI UEDA AND GENJI JIMBO
Department of Chemical Engineering, Nagoya University, Nagoya 464

Key Words: Fluidized Bed, Incipient Fluidization, Elevated Temperature, Adhesive Force, Cluster Formation

A new model describing the effect of the adhesive force of particles on the bed structure in a fluidized bed is proposed. Based on this model, equations for estimating the minimum fluidization bed voidage and gas velocity were analytically derived as functions of the particle size and the adhesive force of particles. From a comparison of theoretical values with experimental values obtained in silica sand beds with various particle sizes at temperatures up to 873 K, the analytical equations were found to give excellent predictions. The predicted values were also found to agree well with the experimental values of bed voidage at ambient conditions by Leva.

Introduction

Although many fluidized bed processes are operated at elevated temperature, correlations developed for the prediction of the minimum fluidization velocity, u_{mf}, are mostly based on experimental work carried out at ambient temperature. In the last decade, some studies dealing with u_{mf} at elevated temperature have been conducted: Desai *et al.*[3] and Doheim *et al.*[4] proposed empirical correlations predicting u_{mf} as a function of temperature. Saxena *et al.*,[9] Svoboda *et al.*[10] and Botterill *et al.*[1] concluded that the application of correlations based on ambient conditions at elevated temperature show marked discrepancies between the observed values of u_{mf} and those predicted with the gas physical properties at the operating temperature. However, no systematic elucidation of the fluidization mechanism at high temperature has been established because of lack of knowledge of the causes of these discrepancies.

In the previous work, u_{mf} and the voidage at incipient fluidization, ε_{mf}, of relatively small particles were examined experimentally at temperatures ranging from 1170 K to 293 K. The authors found that ε_{mf} varies with temperature and that the variation is caused by change in the adhesive force of particles with temperature.[5]

In the present work, based on the previous one, an analytical equation predicting minimum fluidization velocity at elevated temperature is derived by assuming a simple model which describes the relation between the bed voidage and the adhesive force of particles. In addition, the validity and usefulness of this analysis is discussed.

Received August 5, 1985. Correspondence concerning this article should be addressed to R. Yamazaki. N. Ueda is now with Nippon Denso Co., Ltd., Kariya 448.

1. Theory

The following equation[7] has widely been used for estimating minimum fluidization velocity of relatively small particles:

$$u_{mf}=\frac{(\phi_p d_p)^2}{150}\frac{(\rho_p-\rho_f)g}{\mu_f}\frac{\varepsilon_{mf}^3}{1-\varepsilon_{mf}} \tag{1}$$

In this equation, the shape factor of a single particle, ϕ_p, and the bed voidage at incipient fluidization, ε_{mf}, are especially important factors for the estimation of u_{mf}. Wen and Yu[11] have proposed the following equation on the relation between ϕ_p and ε_{mf}.

$$\frac{1}{\phi_p^2}\frac{1-\varepsilon_{mf}}{\varepsilon_{mf}^3}=11 \tag{2}$$

This equation shows that the voidage depends upon the shape factor of particles only. The experimental results of Leva,[8] however, show that ε_{mf} depends not only upon the shape factor but also upon the particle size, d_p, and it increases with decreasing particle size for particles smaller than about 400 μm. Furthermore, the authors showed by experiment that ε_{mf} also depends upon the operating temperature and pointed out that the changes in ε_{mf} with particle size and operating temperature were mainly caused by the change in adhesiveness of particles.[5]

Based on the results mentioned above, an equation predicting u_{mf} at elevated temperature is analytically derived by a newly proposed model describing the

quantitative relation between ε_{mf} and the adhesive force of particles.

1.1 Model presentation

The general concept of the model for predicting ε_{mf} is as follows: In the case of fluidized particles with negligibly small adhesive force compared with their weight, each particle behaves as a single particle. But in the case of fluidized particles with large adhesive force, the particles stick together and behave as clusters consisting of two or more particles. When the supply of fluidizing gas is reduced to the minimum fluidization velocity, these clusters settle down and make a packed bed with relatively loose packing structure, because the clusters have an irregular shape. Thus, it can be assumed that ε_{mf} is expressed by a function of the shape factor of the cluster.

In addition to the general concept, the following assumptions are made:

Assumption 1 It can be assumed that the shape factor of the cluster, Φ, is given by

$$\Phi=\phi_p\cdot\phi_a \tag{3}$$

where ϕ_a is the shape factor of the cluster composed of spherical particles. And it is assumed that the shape of a cluster is expressed by an envelope surface of the surrounding clusters which come in touch with the cluster concerned. The shape of the cluster is illustrated in **Fig. 1**. Then, ϕ_a is expressed as (see **Appendix 1**)

$$\phi_a=\frac{1}{n^{1/3}}\left(1+0.188\frac{n-1}{n}\right) \tag{4}$$

where n denotes the number of particles in a cluster. Combining Eqs. (3) and (4), Φ is expressed as

$$\Phi=\frac{\phi_p}{n^{1/3}}\left(1+0.188\frac{n-1}{n}\right) \tag{5}$$

Assumption 2 At incipient fluidization, the hydrodynamic drag force acting on a cluster, averaged over the total bed, counterbalances the weight of the cluster. A certain difference in the local packing structure of a cluster may yield some deviation in the drag force on the clusters, and therefore, a separating force, F_s, which is proportional to the weight of a cluster. Furthermore, it can be assumed that the separating force, F_s, counterbalances the adhesive force at a contacting point between particles in a cluster. Then

$$F_{ad}=F_s=(\pi/6)kn\rho_p d_p^3 g \tag{6}$$

The following expression for n is obtained from Eq. (6).

$$n=\frac{F_{ad}}{(\pi/6)k\rho_p d_p^3 g} \tag{7}$$

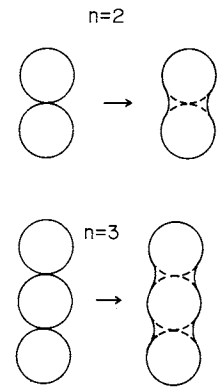

Fig. 1. Illustration of clusters.

Assumption 3 It is assumed that the adhesive force, F_{ad}, is expressed as a following function of particle size and operating temperature.

$$F_{ad}=cf(T)d_p^2 \tag{8}$$

in which $f(T)$ denotes the ratio of the adhesive force at temperature T to that at room temperature. And c denotes a constant which depends upon the materials of the particle itself. (The basis for the dependence of adhesive force on particle size is shown in **Appendix 2**.)

Assumption 4 It is assumed that the following equation, which is analogous to Eq. (2) by Wen and Yu,[11] holds between Φ and $\varepsilon_{mf}^3/(1-\varepsilon_{mf})$.

$$\frac{1}{\Phi^2}\frac{1-\varepsilon_{mf}}{\varepsilon_{mf}^3}=K \tag{9}$$

1.2 Derivation of ε_{mf} and u_{mf} as functions of particle size and temperature

Substitution of Eq. (5) into Eq. (9) gives

$$\frac{\varepsilon_{mf}^3}{1-\varepsilon_{mf}}=\frac{1}{K\phi_p^2}\frac{n^{2/3}}{\left(1+0.188\dfrac{n-1}{n}\right)^2} \tag{10}$$

Since $0.188(n-1)/n\ll 1$,

$$\frac{1}{\left(1+0.188\dfrac{n-1}{n}\right)^2}\doteqdot 1-0.376\left(\frac{n-1}{n}\right)$$

$$=0.624(1+0.603/n) \tag{11}$$

Using the above approximation, Eq. (10) is expressed as follows:

$$\frac{\varepsilon_{mf}^3}{1-\varepsilon_{mf}}=0.624\frac{n^{2/3}}{K\phi_p^2}(1+0.603/n) \tag{12}$$

Designating ε_{mf} at $n=1$ in Eq. (12) by ε_{mfc}, Eq. (12) is expressed as follows:

$$\frac{\varepsilon_{mfc}^3}{1-\varepsilon_{mfc}}=\frac{1}{K\phi_p^2} \tag{13}$$

Elimination of $K\phi_p^2$ from Eqs. (12) and (13) gives the

final expression for the relation between ε_{mf} and n as follows:

$$\left(\frac{\varepsilon_{mf}^3}{1-\varepsilon_{mf}}\right)\Big/\left(\frac{\varepsilon_{mfc}^3}{1-\varepsilon_{mfc}}\right)=0.624n^{2/3}(1+0.603/n) \quad (14)$$

The relation between n and d_p, $f(T)$, can be obtained by substituting Eq. (8) into Eq. (7):

$$n=\frac{cf(T)}{(\pi/6)k\rho_p d_p g} \quad (15)$$

Designating the smallest size of particle which does not form a cluster at room temperature, i.e. the particle size at $f(T)=1$ and $n=1$, by d_{pc}, Eq. (15) is expressed as follows:

$$n=f(T)(d_{pc}/d_p) \quad (16)$$

Substitution of Eq. (16) into Eq. (14) finally leads to the following equations for $\varepsilon_{mf}^3/(1-\varepsilon_{mf})$.

$$\left(\frac{\varepsilon_{mf}^3}{1-\varepsilon_{mf}}\right)\Big/\left(\frac{\varepsilon_{mfc}^3}{1-\varepsilon_{mfc}}\right)=0.624f(T)^{2/3}\left(\frac{d_{pc}}{d_p}\right)^{2/3}\times\left[1+\frac{0.603}{f(T)(d_{pc}/d_p)}\right] \quad (17)$$

for $\quad f(T)(d_{pc}/d_p)\geqq 1 \quad (18)$

while

$$\left(\frac{\varepsilon_{mf}^3}{1-\varepsilon_{mf}}\right)\Big/\left(\frac{\varepsilon_{mfc}^3}{1-\varepsilon_{mfc}}\right)=1 \quad (19)$$

for $\quad f(T)(d_{pc}/d_p)<1 \quad (20)$

Using Eqs. (1), (17) and (19), u_{mf} is expressed as follows for $f(T)(d_{pc}/d_p)\geqq 1$:

$$u_{mf}=\frac{(\phi_p d_p)^2}{150}\frac{(\rho_p-\rho_f)g}{\mu_f}\left(\frac{\varepsilon_{mfc}^3}{1-\varepsilon_{mfc}}\right)\times k_1 f(T)^{2/3}\left(\frac{d_{pc}}{d_p}\right)^{2/3}\cdot\left[1+\frac{k_2}{f(T)(d_{pc}/d_p)}\right] \quad (21)$$

where

$$K_1=0.624, \quad K_2=0.603$$

and for $\quad f(T)(d_{pc}/d_p)<1$:

$$u_{mf}=\frac{(\phi_p d_p)^2}{150}\frac{(\rho_p-\rho_f)g}{\mu_f}\left(\frac{\varepsilon_{mfc}^3}{1-\varepsilon_{mfc}}\right) \quad (22)$$

2. Experimental

A schematic diagram of the experimental apparatus is shown in **Fig. 2**. The bed column, made of stainless steel, was 60 mm in diameter and 500 mm high. A porous plate made of stainless steel was used as a gas distributor.

After particles of known weight were fully fluidized with air from a blower (1), the bed was heated to a scheduled temperature by heaters (6, 8). After the temperature became constant, the air velocity was gradually reduced from that for a fully fluidized state to that for a static bed, and the relation between pressure drop and air velocity was measured. u_{mf} was then determined in the usual way as the point of intersection between the two straight lines on a plot of pressure drop vs air velocity.

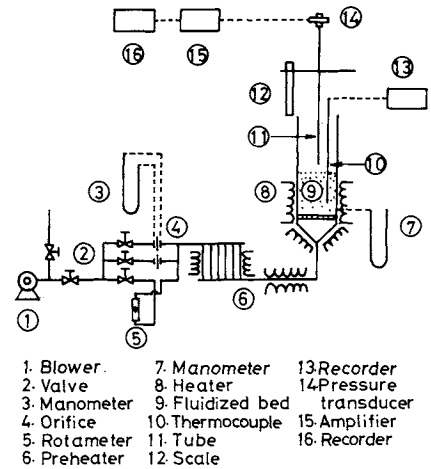

Fig. 2. Schematic diagram of experimental apparatus.

The bed voidage at minimum fluidization, ε_{mf}, was also obtained, by the following procedure: After the bed was kept at minimum fluidization, a 2 mm-i.d. stainless steel tube (11) connected to a pressure transducer (14) was inserted into the bed. The bed surface was identified by detecting a small increase in pressure. ε_{mf} was then obtained from the bed height and the density of the particles used. After u_{mf} and ε_{mf} were measured, the bed was returned to a state of incipient fluidization again in order to traverse a thermocouple (10) in the axial direction of the bed. The temperature differences between the top and bottom of the bed were less than 4% of the prescribed temperature. The particles used were silica sand and their sizes are listed in *Table 1*.

3. Experimental Results

The pressure drop, ΔP, against gas velocity, u, for 210 μm sand is shown in **Fig. 3**. The minimum fluidization velocities, u_{mf}, obtained from Δp vs. u plots are shown in **Fig. 4**. The broken lines in this figure denote the calculated values obtained by assuming the bed voidage to be independent of temperature. The observed values of u_{mf} are much larger than the calculated values in the high-temperature region. The solid lines in this figure are explained in the following section. Observed values of ε_{mf} are also shown in **Fig. 5**. For any particle size, the general tendency is that ε_{mf} decreases with increasing temperature below 400 K and increases with temperature above 400 K. This tendency agrees with the

Table 1. Size of silica sand used

Mean size [μm]	Size range [μm]
418	350–500
296	250–350
210	177–250
149	125–177
105	88–125

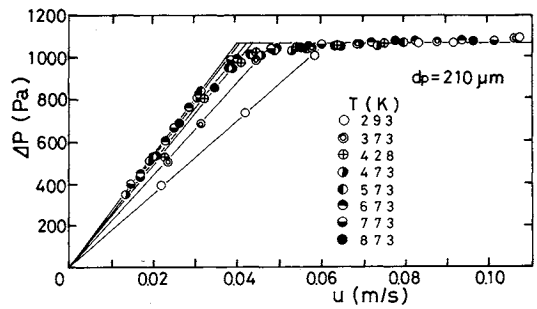

Fig. 3. ΔP vs. u.

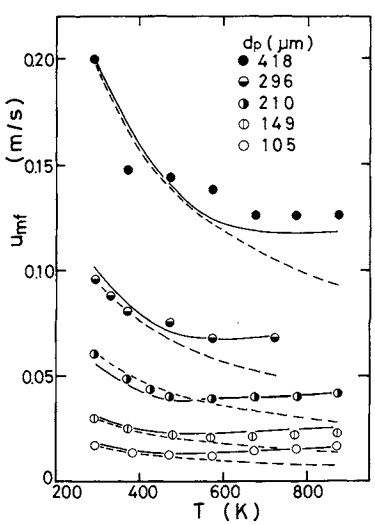

Fig. 4. Variation of u_{mf} with temperature.

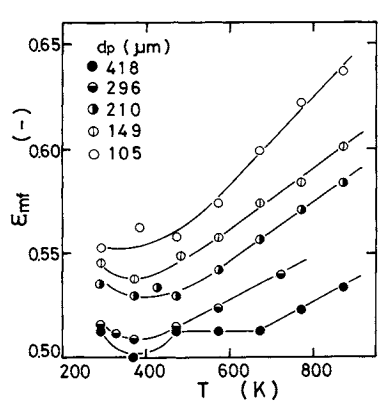

Fig. 5. Variation of ε_{mf} with temperature.

results for a two-dimensional bed.[5]

4. Comparison of Theoretical and Experimental Results

In comparing the observed values of ε_{mf} with Eq. (17) or Eq. (19) derived from the theoretical model, it is necessary to determine the critical particle size, d_{pc}, and the critical bed porosity, ε_{mfc}, as well as the change in adhesive force between particles with temperature, $f(T)$. For $f(T)$, the result of measurement of the adhesive force of a silica sand bed at elevated temperature can be used.[6] The result is shown in **Fig. 6**. From this figure, $f(T)$ is expressed as

$$T \leqq 473\,\mathrm{K};\quad f(T)=1 \tag{23}$$

$$T>473\,\mathrm{K};\quad f(T)=5\times10^{-3}(T-473)+1 \tag{24}$$

For estimating d_{pc}, and ε_{mfc}, $\varepsilon_{mf}^3/(1-\varepsilon_{mf})$ is plotted against $(f(T)/d_p)^{2/3}$ in **Fig. 7**. The relation between these two variables is well expressed by two straight lines. $\varepsilon_{mfc}^3(1-\varepsilon_{mfc})$ can be determined from the horizontal line in this figure. d_{pc} can also be determined by reading the abscissa of the intersection of two lines, putting $f(T)=1$. From this procedure, ε_{mfc} and d_{pc} are determined as

$$\varepsilon_{mfc}=0.516(\varepsilon_{mfc}^3/(1-\varepsilon_{mfc})=0.284)$$

$$d_{pc}=260\,\mu\mathrm{m}(1/d_{pc}^{2/3}=11.4\,\mathrm{cm}^{-2/3})$$

The observed values of ε_{mf} are compared with those predicted by Eqs. (17) and (19) in **Fig. 8**. Close agreement between theoretical and experimental values is seen.

The observed values of u_{mf} can be compared with the theoretical values by the following procedure. To determine the value of ϕ_p in Eqs. (21) and (22), u_{mf} is plotted against $(d_p^2/\mu_f)\cdot(\varepsilon_{mf}^3/(1-\varepsilon_{mf}))$ in **Fig. 9**. This figure shows that Eq. (1) is valid within 10% error and therefore ϕ_p is independent of particle size. The relation shown in Fig. 9 and Eq. (1) gives $\phi_p=0.633$. The solid lines in Fig. 4 show the calculated value of Eqs. (21) and (22) using this value of ϕ_p. The experimental values agree well with the calculated results. To examine the accuracy in estimating u_{mf} with Eqs. (21) and (22), the plot of observed vs. calculated u_{mf} is shown in **Fig. 10**. From the figure, the calculated values correspond within 10% error.

The validity of Eqs. (17) and (19) can be confirmed by applying these equations to Leva's results[8] of ε_{mf} for various particles at ambient temperature.

Putting $f(T)=1$ and assuming $d_{pc}=260\,\mu$m for any kind of particles used, a plot of $(\varepsilon_{mf}^3/(1-\varepsilon_{mf}))/(\varepsilon_{mfc}^3/(1-\varepsilon_{mfc}))$ vs. $0.624(d_{pc}/d_p)^{2/3}[1+0.603/(d_{pc}/d_p)]$ was made with Leva's results. The plot is shown in **Fig. 11**. The observed values are found to agree well with the theoretical values. This also shows that the assumption $d_{pc}=260\,\mu$m is valid and that the adhe-

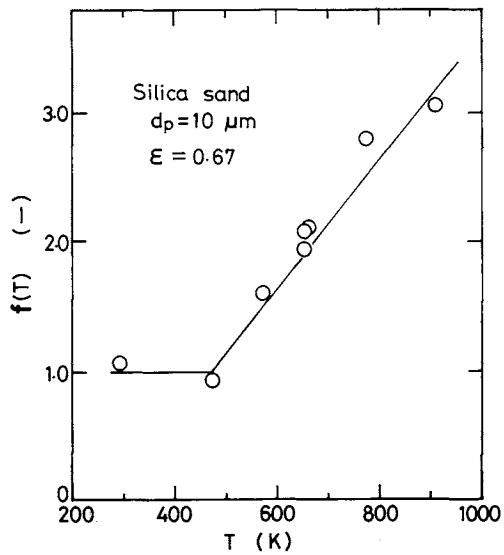

Fig. 6. Variation of adhesive force of silica sand with temperature.

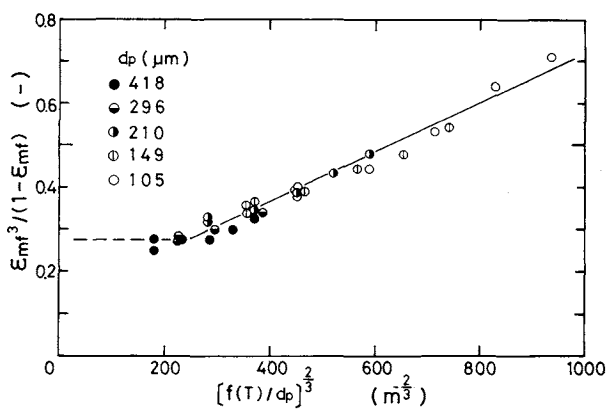

Fig. 7. Plots of $\varepsilon_{mf}^3/(1-\varepsilon_{mf})$ vs. $[f(T)/d_p]^{2/3}$.

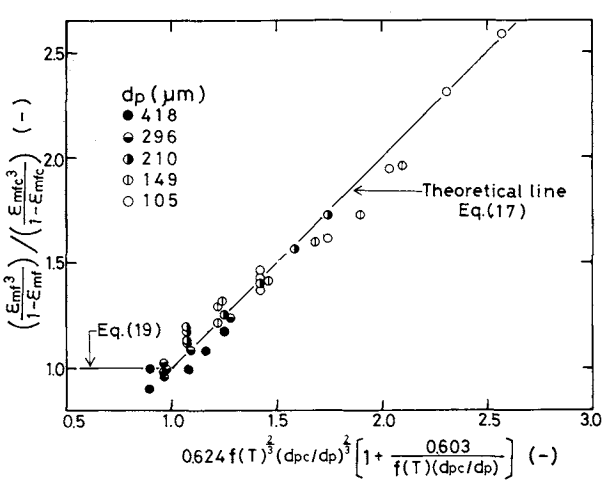

Fig. 8. Comparison of observed ε_{mf} with calculated values.

siveness of these particles is almost the same.

Equation (21) can be transformed into a more convenient form by replacing u_{mf} in Eq. (22) by u_{mfc} and dividing Eq. (21) by Eq. (22); then the following expression for u_{mf} is obtained.

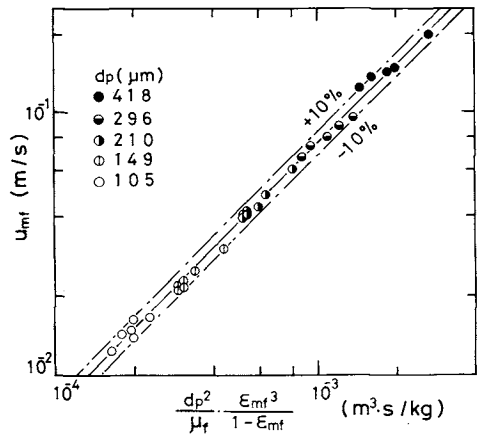

Fig. 9. Plots of u_{mf} vs. $\frac{d_p^2}{\mu_f}\cdot\frac{\varepsilon_{mf}^3}{1-\varepsilon_{mf}}$.

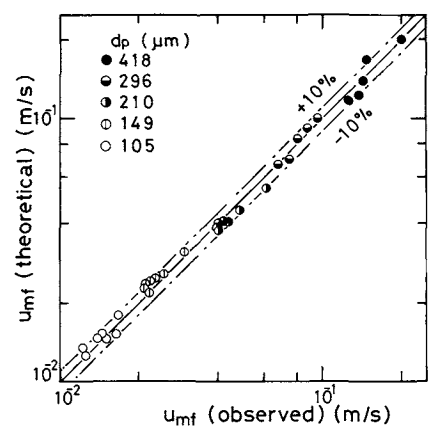

Fig. 10. Comparison of observed u_{mf} with calculated values.

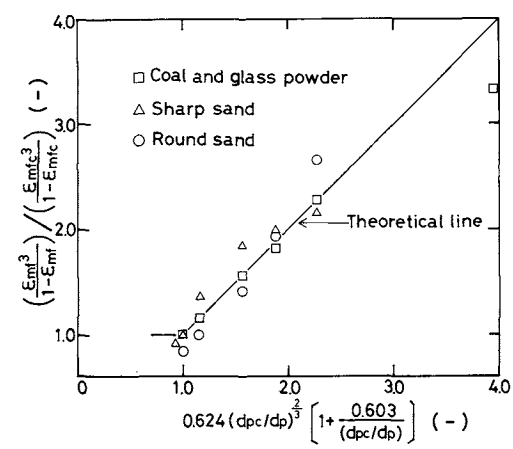

Fig. 11. Comparison of observed ε_{mf}[8] with calculated values.

$$u_{mf}/u_{mfc}=0.624f(T)^{2/3}\left(\frac{d_{pc}}{d_p}\right)^{2/3}\left[1+\frac{0.603}{f(T)(d_{pc}/d_p)}\right] \tag{25}$$

where

$$u_{mfc}=\frac{(\phi_p d_p)^2}{150}\,\frac{(\rho_p-\rho_f)g}{\mu_f}\,\frac{\varepsilon_{mfc}^3}{1-\varepsilon_{mfc}} \tag{26}$$

In the previous paper[12] the following relation was obtained for the various particles under the laminar flow condition.

$$\frac{\phi_p^2}{150}\frac{\varepsilon_{mfc}^3}{1-\varepsilon_{mfc}}=\frac{1}{1200} \tag{27}$$

In this work, the values for ϕ_p and ε_{mfc} are 0.663 and 0.516 respectively. Using these values, $(\phi_p^2/150)(\varepsilon_{mfc}^3/(1-\varepsilon_{mfc}))$ has a value of 1/1200, indicating the validity of the above equation. Substitution of Eq. (27) into Eq. (26) gives

$$u_{mfc}=\frac{(\rho_p-\rho_f)d_p^2 g}{1200\mu_f} \tag{28}$$

u_{mf} can be estimated by using both Eq. (25) and Eq. (28) when particles are strongly adhesive, and using Eq. (28) when the adhesiveness is negligible.

Conclusion

Equations for estimating the minimum fluidization velocity and bed voidage at elevated temperatures were analytically derived from a newly proposed model assuming the formation of clusters consisting of several particles in the bed. It was found that the analytical equation predicts the minimum fluidization velocity within $\pm 10\%$ error.

Appendix 1

First, consider the case of a cluster of two spherical particles. Provided that the cluster has an envelope surface which is formed by the group of spheres (O_3, O_4, $\cdots$) contacting two spheres (O_1, O_2), it is expressed as the solid ADECBC'E'D' as shown in **Fig. A-1**. The shape factor of the cluster can be obtained from its volume and surface area. Using an x, y coordinate system with origin at H as shown in the figure, the equation of the circle O_4 is expressed as

$$x^2+(y-\sqrt{3}R)^2=R^2 \tag{A-1}$$

where R denotes the radius of the sphere. Then the volume of the solid ABCD, v, is given by

$$v=\pi\int_0^{R/2} y^2dx=\frac{29-4\sqrt{3\pi}}{24}\pi R^3$$
$$=0.302\pi R^3 \tag{A-2}$$

The volume of the solid DHC, v', is given by

$$v'=5/24\pi R^3 \tag{A-3}$$

Then the volume of the solid AHBCED is expressed as

$$V=V_o+v-v'$$
$$=V_o(1+\Delta v) \tag{A-4}$$

where

$$V_o=(4/3)\pi R^3$$
$$\Delta v=0.0705$$

The surface area of the solid ABCD, s, is expressed by the following equation.

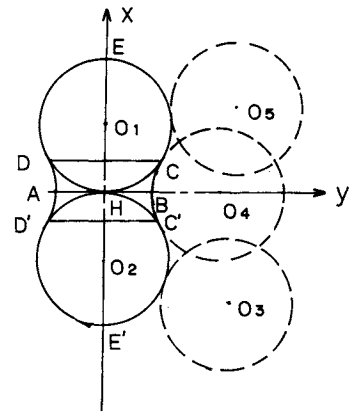

Fig. A-1. Definition of shape of cluster.

$$s=2\pi\int_0^{R/2} y\sqrt{1+\left(\frac{dy}{dx}\right)^2}dx \tag{A-5}$$

From Eqs. (A-1) and (A-5),

$$s=2\left(\frac{\sqrt{3}}{6}\pi-\frac{1}{2}\right)\pi R^2$$
$$=0.812\pi R^2 \tag{A-6}$$

The surface area of the solid DHC, s', is given by

$$s'=\pi R^2 \tag{A-7}$$

Equations (A-6) and (A-7) give the following expression for the surface area of the solid ABCED, S.

$$S=4\pi R^2-s'+s$$
$$=S_o(1-\Delta s) \tag{A-8}$$

where

$$S_o=4\pi R^2$$
$$\Delta s=0.047$$

In the case of the cluster comprising n particles, the volume, V_n, and surface area, S_n of the cluster, are given by the following expressions respectively.

$$V_n=nV_o+2(n-1)V_o\Delta v$$
$$=nV_o\left\{1+2\left(\frac{n-1}{n}\right)\Delta v\right\} \tag{A-9}$$

$$S_n=nS_o-2(n-1)S_o\Delta s$$
$$=nS_o\left\{1-2\left(\frac{n-1}{n}\right)\Delta s\right\} \tag{A-10}$$

Designating the diameter and the surface area of the sphere having the volume of the cluster by D_e and S_s respectively, then

$$S_s=\pi D_e^2 \tag{A-11}$$

From Eq. (A-9),

$$D_e=d_p n^{1/3}\left\{1+2\left(\frac{n-1}{n}\right)\Delta v\right\}^{1/3} \tag{A-12}$$

Substituting Eq. (A-12) into Eq. (A-11),

$$S_s=\pi d_p^2 n^{2/3}\left\{1+2\left(\frac{n-1}{n}\right)\Delta v\right\}^{2/3} \tag{A-13}$$

The shape factor of the cluster, ϕ_a, can be defined by the following expression:

$$\phi_a=\frac{\text{(Surface of the sphere having the volume of the cluster)}}{\text{(Surface of the cluster)}}$$

$$=S_s/S_n \tag{A-14}$$

Substituting Eqs. (A-10) and (A-13) into Eq. (A-14),

$$\phi_a=\frac{\left\{1+2\left(\frac{n-1}{n}\right)\Delta v\right\}^{2/3}}{n^{1/3}\left\{1-2\left(\frac{n-1}{n}\right)\Delta s\right\}} \tag{A-15}$$

The following approximate equation holds for small values of Δv and Δs.

$$\frac{\left\{1+2\left(\frac{n-1}{n}\right)\Delta v\right\}^{2/3}}{1-2\left(\frac{n-1}{n}\right)\Delta s}$$

$$\doteqdot\left\{1+2\left(\frac{n-1}{n}\right)\Delta s\right\}\left\{1+\frac{4}{3}\left(\frac{n-1}{n}\right)\Delta v\right\}$$

$$\doteqdot 1+\left(\frac{n-1}{n}\right)\left\{2\Delta s+\frac{4}{3}\Delta v\right\}=1+0.188\left(\frac{n-1}{n}\right) \tag{A-16}$$

Substitution of Eq. (A-16) into Eq. (A-15) gives Eq. (4).

Appendix 2

Although there have been few experimental works on the measurement of the adhesive force of relatively large particles used in fluidized beds, Buysman and Peersman[2] obtained the adhesive force of fluidizing particles from experiments on the stability of ceilings in a fluidized bed. An example of their experimental data is shown in **Fig. A-2**. The figure shows that the adhesive force is proportional to the square of the particle size.

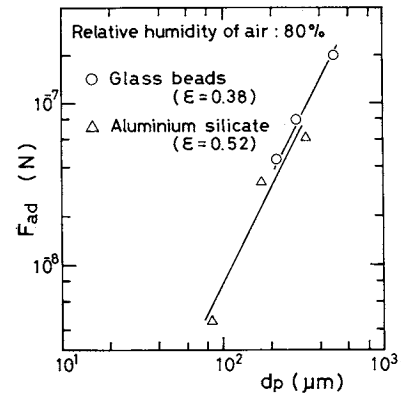

Fig. A-2. Dependence of adhesive force on particle size (results of Buysman *et al.*[2] were replotted).

Nomenclature

c	=	constant defined by Eq. (8)	[N/m^2]
d_p	=	particle diameter	[μm,m]
F_{ad}	=	adhesive force of particle	[N]
F_s	=	separating force on particle	[N]
$f(T)$	=	ratio of adhesive force at elevated temperature to that at room temperature	[—]
g	=	acceleration of gravity	[m/s^2]
K	=	constant defined by Eq. (9)	[—]
k	=	ratio of separating force on particle to weight of cluster	[—]
n	=	number of particles composing a cluster	[—]
ΔP	=	pressure drop	[Pa]
T	=	temperature	[K]
u	=	gas velocity	[m/s]
u_{mf}	=	minimum fluidization velocity	[m/s]
ε_{mf}	=	bed voidage at incipient fluidization	[—]
μ_f	=	gas viscosity	[Pa·s]
ρ_f	=	gas density	[k$_g$/m^3]
ρ_p	=	particle density	[k$_g$/m^3]
ϕ_a	=	shape factor of a cluster composed of spherical particles (defined by Eq. (3))	[—]
ϕ_p	=	shape factor of single particle	[—]
Φ	=	shape factor of a cluster (defined by Eq. (3))	[—]

〈Subscript〉

c	=	critical state where clusters are formed

Literature Cited

1) Botterill, J. S. M., Y. Teoman and K. R. Yuregir: *Powder Technology*, **31**, 101 (1982).
2) Buysman, P. J. and G. A. L. Peersman: Proc. Intl. Symp. Fluidization, Eindhoven, p. 38 Netherland Univ. Press (1967).
3) Desai, A., H. Kikukawa and A. H. Pulsifer: *Powder Technology*, **16**, 143 (1977).
4) Doheim, M. A. and C. N. Collinge: *Powder Technology*, **21**, 289 (1978).
5) Hong, G. H., R. Yamazaki, T. Takahashi and G. Jimbo: *Kagaku Kogaku Ronbunshu*, **6**, 557 (1980).
6) Jimbo, G., R. Yamazaki and G. H. Hong: Reports of the Asahi Glass Foundation for Industrial Technology, **38**, 123 (1981).
7) Kunii, D. and O. Levenspiel: "Fluidization Engineering," John Wiley and Sons, New York (1969).
8) Leva, M.: "Fluidization," McGraw-Hill, New York (1959).
9) Saxena, S. C. and G. J. Vogel: *Trans. Inst. Chem. Engrs.* (London), **55**, 184 (1977).
10) Svoboda, K. and M. Hartman: *Ind. Eng. Chem. Process Des. Dev.*, **20**, 319 (1981).
11) Wen, C. Y. and Y. H. Yu: *AIChE J.*, **12**, 610 (1966).
12) Zheng, Z., R. Yamazaki and G. Jimbo: *Kagaku Kogaku Ronbunshu*, **11**, 115 (1985).